Atmos. Chem. Phys. Discuss., 11, 31137–31158, 2011
www.atmos-chem-phys-discuss.net/11/31137/2011/
doi:10.5194/acpd-11-31137-2011

Atmospheric Chemistry and Physics Discussions

A new approach to estimate pollutant emissions based on trajectory modelling and its application in the North China Plain

W. Y. Xu[1], C. S. Zhao[1], P. F. Liu[1], L. Ran[1], N. Ma[1], Z. Z. Deng[1], W. L. Lin[2], P. Yan[2], and X. B. Xu[2]

[1]Department of Atmospheric and Oceanic Sciences, School of Physics, Peking University, Beijing, China
[2]Key Laboratory for Atmospheric Chemistry, Centre for Atmosphere Watch and Services, Chinese Academy of Meteorological Sciences, China Meteorological Administration, Beijing, China

Received: 12 July 2011 – Accepted: 14 November 2011 – Published: 24 November 2011

Correspondence to: C. S. Zhao (zcs@pku.edu.cn)

Published by Copernicus Publications on behalf of the European Geosciences Union.

Abstract

Emission information is crucial for air quality modelling and air quality management. In this study, a new approach based on the understanding of the relationship between emissions and measured pollutant concentrations has been proposed to estimate pollutant emissions and source contributions. The retrieval can be made with single point in-situ measurements combined with backward trajectory analyses. The method takes into consideration the effect of meteorology on pollutant transport when evaluating contributions and is independent of energy statistics, therefore can provide frequent updates on emission information. The spatial coverage can be further improved by using measurements from several sites and combining the derived emission fields. The method was applied to yield the source distributions of black carbon (BC) and CO in the North China Plain (NCP) using in-situ measurements from the HaChi (Haze in China) Campaign and to evaluate contributions from specific areas to local concentrations at the measurement site. Results show that this method can yield a reasonable emission field for the NCP and can directly quantify areal source contributions. Major BC and CO emission source regions are Beijing, the western part of Tianjin and Langfang, Hebei, with Tangshan being an additional important CO emission source area. The source contribution assessment suggests that, aside from local emissions in Wuqing, Tianjin and Hebei S, SW ($d < 100$ km) are the greatest contributors to measured local concentrations, while emissions from Beijing contribute little during summertime.

1 Introduction

Emission inventories are crucial for the modelling of gaseous and particulate pollutants and for the establishment of air quality management strategies, for which both local emissions and transport of pollutants need to be considered.

A fundamental problem of air quality modeling is that, it depends on the assumption that emission inventories are accurate. Chemical transport models are very sensitive

ACPD
11, 31137–31158, 2011

to emission inventories. Different emission inventories may results in vastly different modelling outcomes (Ma et al., 2004). The most common approaches of deriving emissions are bottom-up and top-down inversion methods. Bottom-up methods are based on energy statistics, which bear large uncertainties and cannot be easily updated (Zhang et al., 2009). Emissions may have large spatial and temporal variations, due to new policies and the rapid development, especially in developing countries such as China. Top-down techniques use atmospheric observations (i.e. satellite observations) and chemistry transport models together with prior emissions to derive optimized emissions (Lin et al., 2007). However, both satellite data and air quality models usually exhibit large uncertainties. Out-dated or inaccurate emission inventory poses a profound problem for air quality modeling and may result in wrong implications for future emission controls. Therefore, alternative approaches need to be developed, so that emission inventories can be updated or corrected.

Efforts in improving the temporal resolution were made by combining air quality measurements with trajectory analyses to yield source distributions. Early methods were mainly based on classification or clustering of trajectories (Miller, 1981; Moody and Samson, 1989; Harris and Kahl, 1990), which could only roughly identify sectors associated with high pollution. Although such methods were not able to yield the spatial distribution of pollutant sources, they were still often used to distinguish different air masses and their accompanied pollutant concentrations (Lin et al., 2009; Tang et al., 2009) or to identify possible source regions on a larger scale (Liu et al., 2009). Ashbaugh (1983) and Ashbaugh et al. (1985) developed a statistical method that calculates the accumulated residence times of all trajectories within cells of a grid separately for a subset of high pollution events (resulting in a partial residence time t) and for the whole data set (resulting in a residence time T), with the ratio t/T indicating the frequency of trajectories passing over a certain grid and being associated with high concentrations at the receptor site. This method was further developed into the Potential Source Contribution Function (PSCF) analysis, which was defined as:

ACPD
11, 31137–31158, 2011

$$\mathrm{PSCF}(i,j) = \frac{m(i,j)}{n(i,j)}, \quad (1)$$

where $n(i,j)$ is the total number of endpoints falling with in the grid (i,j), and $m(i,j)$ is the subset of endpoints that are on trajectories associated with concentrations above a certain criterion. In recent years, the PSCF analysis has been widely applied to identify possible pollutant source regions (Lucey et al., 2001; Arabegum et al., 2005). However, it can only yield a probability distribution of source regions and cannot quantify the source strength. Seibert et al. (1994) suggested calculating a logarithmic mean concentration for each grid on the domain of the trajectory analyses following the equation:

$$\bar{C}_{mn} = \frac{1}{\sum_{l=1}^{M} \tau_{mnl}} \sum_{l=1}^{M} \log(c_l)\tau_{mnl}, \quad (2)$$

where m and n are indices of the horizontal grid, l is the index of the trajectory, M the total number of trajectories, c_l the concentration at the receptor site at the time upon which trajectory l arrives and τ_{mnl} the residence time of trajectory l in grid (m,n). This method made it easier to evaluate uncertainties of the outcome. Stohl et al. (1996) improved the method by using $\bar{C}_{mn}$ as a first guess, $10^{C_{mn}(i)/\bar{C}_{mnl}}$ $(i = 1,\ldots,N_l$, N_l being the number of grids on trajectory $l)$ as a weighting factor for each trajectory, and iterating the processes until the average difference between the concentration fields of two successive iterations is below 0.5 %. Such concentration field analyses are often used to detect possible plumes or yielding the regional distribution of pollutants (de Foy et al., 2007). Stohl's method solved the problem that the Seibert et al. method attributes the receptor concentration c_l equally to all parts of trajectory l, however, iteration techniques often face the problem of convergence and "hot spots" on the first guess field are amplified while information of the other sections on the same trajectories with the "hot spots" easily get lost through iterations. Another problem with this technique is that it yields a logarithmic mean concentration field and one cannot directly derive emission rates from it, or quantify the contributions of source regions to

ACPD
11, 31137–31158, 2011

the receptor site. Also, this method does not consider the influence of the boundary layer on pollutant concentrations.

A new method based on the understanding of the relationship between emissions and measured pollutant concentrations will be presented in this work, mainly focusing on the transport of pollutants within the planetary boundary layer (PBL). The application of the new method on deriving black carbon (BC) and CO emission fields and assessing source contributions will also be shown.

2 Methodology

2.1 Site and measurements

Measurements of BC and CO were conducted at the Wuqing Meteorological Station, located at a suburban district between Beijing and Tianjin and surrounded by Hebei Province. This site has proved to be highly representative of the overall pollution level of the polluted NCP region and a favourable spot for observing transport of air pollutants (Xu et al., 2011).

A Multi-angle Absorption Photometer (MAAP Model 5012, Thermo, Inc., Waltham, MA USA) was employed to measure BC mass concentration in unit of $\mu g\, m^{-3}$, while CO was measured with a gas filter correlation analyser (TE 48C, Thermo Environmental Instruments Inc., USA), and recorded as 1-min average mixing ratios by volume (ppbv). Meteorological variables were obtained by an Automatic Weather Station installed at the Wuqing Meteorological Station. Details on the measurement site, instruments, data maintenance and calibration are described by Ma et al. (2011) and Xu et al. (2011).

2.2 WRF simulations

The ARW (Advanced Research WRF) model is used to generate high resolution meteorology fields for the backward trajectory study with the Hybrid Single

ACPD
11, 31137–31158, 2011

Particle Lagrangian Integrated Trajectory (HYSPLIT) model. An 18 km/6 km two-way nested grid was applied in the simulation, with the outer domain covering an area of 1500 km × 1500 km large (Fig. 1). The model physics options used are WRF Single Moment Class 3 (WSM3) for microphysics parameterization, Rapid Radiative Transfer Model (RRTM) scheme (Mlawer et al., 1997) for longwave radiation processes, Dudhia scheme for short wave radiation (1989), 5-layer thermal diffusion for land surface processes (Dudhia, 1996), Yonsei University non-local scheme for boundary layer parameterization (Hong et al., 2006), Kain-Fritsch scheme (Kain and Fritsch, 1993) for cumulus parameterization. The simulation period is from 11 July to 14 August 2009. The period was split into several runs, with each run simulating 3 days and 12 h. The model was initialized every 3 days at 12:00 UTC and integrated over 84 h. The first 12 h of each run was discarded due to model spin-up. The initial and boundary conditions required for ARW model integrations were adopted from National Centers of Environmental Prediction (NCEP), which were updated every 6 h.

2.3 Backward trajectory calculations and cluster analyses

The HYSPLIT model (version 4) from NOAA Air Resources Laboratory http://ready.arl.noaa.gov/HYSPLIT.php; Draxler and Hess, 1998) was used for the backward trajectory analyses, applying only the ARW output of the inner domain, which has a spatial resolution of 6 km × 6 km and a temporal resolution of 1h. The trajectory endpoint is set to 39.38° N and 117.02° E with a height of 50 m a.g.l. 48 h backward trajectories were calculated at a 1 h interval from 13 July to 14 August 2009.

For each backward trajectory, the direction of each time-step was calculated and a vector mean value was taken as the average direction of this trajectory. Then, based on the average directions and the PBL residence time (Sect. 2.4), the trajectories were clustered into 8 groups.

ACPD
11, 31137–31158, 2011

2.4 Methodology of emission retrieval and areal source contribution assessment

Assuming that pollutant concentrations are well mixed within the PBL, emissions into a certain air mass can be estimated as the concentrations divided by the residence time. If we further presumed that all grids on the same trajectory l share the same pollutant concentrations, we would yield a uniform emission factor for all grids on l:

$$E_l = C_l / T_l \,, \tag{3}$$

where C_l stands for local concentrations upon arriving time of l at the receptor site, T_l is the residence time of l in the PBL. Trajectories cross each other's paths, and each grid (m,n) will be associated with multiple emission values, by averaging them, we get the mean emission rate of (m,n):

$$\bar{E}_{mn} = \overline{\sum_{l=1}^{M} C_l / T_l}^{mn} \,, \tag{4}$$

where M is the total number of trajectories. Considering that is might be unrealistic to assume that all grids on l have the same emission rate, especially when l travels a long distance, the method can be improved by introducing a weighting factor W:

$$W_{mn} = \frac{F_{mn}}{\bar{F}_{mnl}} \,, \tag{5}$$

where F can be the field of any variable that could serve as a priori to the emission field analyses, e.g. population, NO_2 column distribution or previous emission inventories. $\bar{F}_{mnl}$ is the average value of F for the grids (m,n) that l travels over. In this study the 2006 INTEX-B emission inventories (Zhang et al., 2009) were interpolated into a finer grid and applied as the first guess fields for BC and CO emissions (Fig. 4a1,b1). Finally, the average emission field can be acquired by:

$$\bar{E}_{mn} = \overline{\sum_{l=1}^{M} W_{mn} \cdot C_l / T_l}^{mn} \,. \tag{6}$$

ACPD
11, 31137–31158, 2011

The method used to determine the residence time of trajectory l is shown in Fig. 2. The nighttime (20:00–08:00 LT) PBL height is set as 300 m, while the daytime (08:00–20:00 LT) PBL height is set as 1000 m. We start at the time upon which l arrives at the receptor site (t_1) and go back in time, for each time step of l, it is first to be determined whether it is daytime or night time, then according to the above set PBL height, it is judged whether the air parcel is still in the PBL. This is proceeded until the first time step where l reaches the PBL height (t_h). The PBL residence time T_l is thus determined as:

$$T_l = t_1 - t_h \,. \tag{7}$$

With the calculated mean emission field, the pollutant contributions of specific source regions to the receptor site can be easily assessed. The receptor site concentration contribution of each grid can be calculated as:

$$\bar{P}_{mn} = \bar{E}_{mn} \cdot \tau_{mn} \,, \tag{8}$$

where τ_{mn} is the total residence time of all trajectories within the PBL in grid (m,n).

In this study, the concentration contributions of local emissions in Wuqing and the transport contributions of Beijing, Tianjin and Hebei Province were assessed. Instead of τ_{mn}, the average daily residence time (total residence time divided by the days of the trajectory analyses (32 days)) was applied to acquire an average daily concentration contribution. For each source region evaluated, the mean, minimum and maximum daily concentration contributions $\bar{P}_{mean}$, $\bar{P}_{min}$ and $\bar{P}_{max}$ were acquired by averaging $\bar{P}_{mn}$ over the grids or taking the minimum and maximum grid value within the bounds of the region. Accordingly, mean concentration contribution fractions could be calculated by:

ACPD
11, 31137–31158, 2011

$$\bar{f}_i = \frac{\bar{P}_i}{\sum_i \bar{P}_i} \times 100\%, \quad i = 1, \ldots, 8, \tag{9}$$

where i stands for the different regions assessed in this study.

This method of emission retrieval is straightforward and can be accomplished based on single site measurements. Traditional bottom-up emission estimates depend highly on energy statistics, which take a long time to be updated and are crucial to the accuracy of emission inventories (Akimoto et al., 2006). Our retrievals can be frequently updated benefitting from the high temporal resolutions of ground measurements. The method is widely applicable for pollutants with longer lifetimes than the time used to constrain trajectories. It can be used for analyses of seasonal variations in emissions or areal contributions, if provided long-term monitoring data. It should be noted that by only taking into account trajectories within the PBL, the emission field is restricted to a limited distance range. However, improvements can be made by using measurements from several sites, which would compensate for the lack in spatial coverage.

3 Results and discussion

3.1 Trajectory frequency analyses

Figure 3 shows all the trajectories divided into 8 clusters, according to its direction and PBL residence time. During the measurement period, most trajectories came from the S–W (55.0 %), with a dominant part showing PBL residence time shorter than 24 h (49.1 %). Trajectories mostly come from Southern Hebei, while a few of them originate from the northern edge of Henan Province or the western edge of Shandong Province. S–E, with an occurrence frequency of 24.4 %, is the second most dominant direction of backward trajectories. Trajectories with PBL residence time greater than 24 h appear most frequently (11.0 %) under this direction. Generally, they travel from the Bohai Sea over the industrial region and the inner city of Tianjin before arriving at the site; a few of

ACPD
11, 31137–31158, 2011

them originate from Shandong Province or the Yellow Sea. Trajectories from N–E and N–W are mostly short in distance and residence time. The N–E cluster travels over the NE part of Hebei, while the N–W cluster travels over Beijing.

3.2 BC and CO emissions in the NCP

The emissions of BC and CO in China were assessed by Streets et al. (2001) for the year 1995 and by Zhang et al. (2009) for the year 2006. BC and CO exhibit important influences on the climate and human health (Cooke and Wilson, 1996; Ackerman et al., 2000), they both show increased emissions in 2006 compared to inventories in 1995. Many uncertainties still exist in the inventories, which need to be improved. BC aerosol and CO are both mainly released anthropogenically from fossil fuel combustion and biomass burning and naturally from forest fires (Jacobson, 2001). BC has a lifetime of one (±1) week (Ramanathan and Carmichael, 2008), while CO has a lifetime of 30–90 days on the global scale of the troposphere (Seinfeld and Pandis, 2006).

Figure 4a3 shows the average emission of BC, retrieved with the new method (Sect. 3). Since trajectories are only used to the point where they reach out of the boundary layer, only the emission information of a limited region could be obtained. Average BC emissions are high in Tianjin and Beijing Municipality, which agrees well with the INTEX-B emission distribution. The greatest maximum value was found in Beijing (Table 1), with 2.60 $\mu g\,m^{-3}\,h^{-1}$, while the Tianjin area shows a maximum value of 1.41 $\mu g\,m^{-3}\,h^{-1}$. Langfang city, which is located between Beijing and Tianjin, also shows high emission rates (1.62 $\mu g\,m^{-3}\,h^{-1}$), which could not be found in the INTEX-B emission distribution. The south-western part of Hebei shows several high centres of BC emissions in the 2006 emissions, which were, however, not that significant in this study. A possible reason might be that trajectories passing over South Hebei have travelled a long distance before arriving at Wuqing, with most of them having long PBL residence times, thus resulting in relatively lower emission values according to Eq. (6). The representativeness of the average emission field derived by this method might decrease, for locations that are too far away in distance.

ACPD
11, 31137–31158, 2011

Figure 4b3 shows the calculated average CO emission field. Average CO emissions are most prominent in downtown Beijing and Tianjin, with a spatial maximum of 368.35 and 249.06 ppb h^{-1}, respectively. Langfang and Tangshan (Hebei (NE)) also revealed very high emission values, with maximum values reaching 189.29 and 234.52 ppb h^{-1}, respectively. The high centre of average emissions in Tangshan and Langfang are more pronounced than that estimated by the INTEX-B inventory, while those in SW Hebei are not that obvious in comparison.

Comparing the results before (Fig. 4a2,b2) and after (Fig. 4a3,b3) applying the INTEX-B inventory as weighting factor, it can be discerned that even without using any weighting factor, the method is able to derive a reasonable emission field. Using a priori field to weight the trajectories helps to eliminate the noise, especially the high values over oceans.

Altogether, for atmospheric pollutants that have lifetimes longer than the time used to constrain trajectories, the emissions derived with the new approach are reasonable. The spatial resolution of the retrieval might be improved either by applying higher spatial resolution mesoscale modelling or by replacing the simple backward trajectory model with more complicated trajectory models including dispersion processes. The spatial coverage and the accuracy of the retrieval can be increased by using data from a network of stations. This method can be widely applied to ground measurements all around the world and can be used in various senses. Emission inventories require extensive effort and time for wide range data collection, which often cannot keep up with the rapid changes in emissions of developing countries. This method provides a way to update and correct previous inventories. Also, it can be used to analyse seasonal variations in emissions using long-term pollutant monitoring results.

However, knowing only the distribution of emissions is not enough for the establishment of pollution control strategies. The concentration contribution of source regions to local pollution levels is even more crucial and will be discussed in the next section.

ACPD
11, 31137–31158, 2011

3.3 Areal source contribution assessment

High emission centres might not exert great influences on local pollution levels, if air masses hardly travel over them, whereas other locations with comparatively insignificant emissions may have unnegligible influences, because they are often on the travel path. Hence it is the meteorology, upon which the concentration contributions of various emission source regions depend.

Table 2 summarizes the source contributions of Beijing, Tianjin (excluding Wuqing) and Hebei to local BC and CO concentrations in Wuqing and corresponding contribution fractions. Local BC emissions in Wuqing contribute 17.05–86.07 % to local concentrations, with mean daily concentration contributions being 5.69 $\mu g\,m^{-3}$, making it the most dominant source contributor. The BC emissions in Tianjin, Langfang, Hebei S (within 100 km distance to Wuqing, further on referred to as $d < 100$ km) and Hebei SW ($d < 100$ km) also exert considerable influences on local BC concentrations, contributing on average 15.75, 11.27, 10.27 and 9.81 %, respectively. Maximum concentration contributions can reach up to 12.30, 2.26, 4.51 and 3.16 $\mu g\,m^{-3}$, accounting for 36.85, 6.78, 13.52 and 9.47 % of the total concentration, respectively. Although Beijing showed high emission values, its mean contribution to BC concentrations in Wuqing is low (0.41 %).

For CO, similar results could be found. Local CO emissions in Wuqing contribute 25.83–90.89 % to local concentrations, with mean daily concentration contributions being 1751.69 ppb. Tianjin and Hebei SW ($d < 100$ km) contribute on average 420.73 and 252.10 ppb to local CO concentrations, taking up 14.09 and 8.44 % of the total. Maximum contribution fraction of those two regions can reach 33.91 and 13.36 %. Hebei (Langfang) and Hebei S ($d < 100$ km) contribute on average 214.76 (7.19 %) and 186.13 ppb (6.23 %), which is also a considerable amount. The contribution of Beijing is minor in comparison.

In all, areal source contribution assessments could be simply made based on the derived emissions and the residence time of trajectories. Results are in accordance with the conclusions from previous work (Xu et al., 2011).

ACPD
11, 31137–31158, 2011

4 Conclusions

In this study, a new method for air pollutant emission retrieval has been proposed and applied to estimating the source distributions and areal source contributions of BC and CO in the North China Plain.

The retrieval is accomplished based on single point in-situ measurements combined with backward trajectory analyses. The method can easily update emissions in comparison to traditional bottom-up approaches. With long-term pollutant concentration monitoring data, seasonal and inter-annual variations in emissions can be analysed. In comparison with potential source contribution function techniques, which can only provide possible source locations, our method can provide an emission strength distribution. It can also be directly used to evaluate areal source contributions. All of the above information is crucial for setting up air quality management strategies and policies. It should be noted that, by only taking into account trajectories within the PBL, the emission retrieval is restricted to a limited range in space. However, improvements can be made by using measurements from several sites and combining the results, which would compensate for the lack in spatial coverage and the accuracy of the retrieval. The horizontal resolution of the retrieval might be improved either by applying higher spatial resolution mesoscale modelling or by replacing the simple backward trajectory model with more complicated trajectory models including dispersion processes.

The method was applied to calculate BC and CO emissions using measurements from the HaChi Campaign. Results show similar emission distribution patterns as the 2006 INTEX-B results. Major BC emission sources are Beijing, the western part of Tianjin and Langfang. Major CO emission sources are similarly distributed as that of BC, with Tangshan being an additional important emission source. The retrieved emission rates in Langfang are more pronounced those in the INTEX-B emissions, suggesting an underestimation in the previous inventory. Areal source contribution assessments suggest that, aside from local emissions in Wuqing, emissions from Tianjin and Hebei south, southwest ($d < 100$ km) are the greatest contributors to measured

ACPD
11, 31137–31158, 2011

local concentrations. Although Beijing shows large emission rates, it contributes little to local concentrations during summertime, due to dominating southerly wind directions, which agrees with previous results from Xu et al. (2011).

Acknowledgements. We gratefully thank the staff of the Wuqing Meteorological Station for their logistic support. Funds for this research were provided by the National Natural Science Foundation of China Project 40875001 and 40775074, the 973 Program (2011CB403402), and the Basic Research Fund of Chinese Academy of Meteorological Sciences (2008Z011).

References

Ackerman, A. S., Toon, O. B., Stevens, D. E., Heymsfield, A. J., Ramanathan, V., and Welton, E. J.: Reduction of tropical cloudiness by soot, Science, 288, 1042–1047, 2000.

Akimoto, H., Ohara, T., Kurokawa, J., and Horii, N.: Verification of energy consumption in China during 1996–2003 by using satellite observational data, Atmos. Environ., 40, 7663–7667, 2006.

Arabegum, B., Kim, E., Jeong, C., Lee, D., and Hopke, P.: Evaluation of the potential source contribution function using the 2002 Quebec forest fire episode, Atmos. Environ., 39(20), 3719–3724, 2005.

Ashbaugh, L. L.: A statistical trajectory technique for determining air pollution source regions, J. Air Pollut. Control. Ass., 33, 1096–1098, 1983.

Cooke, W. F. and Wilson, J. N.: A global black carbon aerosol model, J. Geophys. Res., 101, 19395–19409, 1996.

de Foy, B., Lei, W., Zavala, M., Volkamer, R., Samuelsson, J., Mellqvist, J., Galle, B., Martínez, A.-P., Grutter, M., Retama, A., and Molina, L. T.: Modelling constraints on the emission inventory and on vertical dispersion for CO and SO_2 in the Mexico City Metropolitan Area using Solar FTIR and zenith sky UV spectroscopy, Atmos. Chem. Phys., 7, 781–801, doi:10.5194/acp-7-781-2007, 2007.

Draxler, R. R. and Hess, G.D: An overview of the HYSPLIT_4 modelling system for trajectories, dispersion and deposition, Aust. Meteorol. Mag., 47, 295–308, 1998.

Dudhia, J.: Numerical study of convection observed during winter monsoon experiment using a mesoscale two-dimensional model, J. Atmos. Sci., 46, 3077– 3107, 1989.

ACPD

11, 31137–31158, 2011

Dudhia, J.: A multi-layer soil temperature model for MM5, Preprint from the Sixth PSU/NCAR Mesoscale Model Users' Workshop, 1996.
Harris, J. M. and Kahl, J. D.: A descriptive atmospheric transport climatology for the Mauna Loa Observatory, using clustered trajectories, J. Geophys. Res., 95, 13651–13667, 1990.
Hong, S. Y., Noh, Y., and Dudhia, J.: A new vertical diffusion package with explicit treatment of entrainment processes, Mon. Weather Rev., 134, 2318–2341, 2006.
Kain, J. S. and Fritsch, J. M.: Convective parameterization for mesoscale models: the Kain-Fritsch scheme, the representation of cumulus convection in numerical models, edited by: Emanuel, K. A. and Raymond, D. J., Am. Meteorol. Soc., Vol. 246, Boston MA, USA, 1993.
Lin, Y., Zhao, C., Peng, L., and Fang, Y.: A new method to calculate monthly CO emissions using MOPITT satellite data, Chinese Sci. Bull., 52(18), 2551–2558, 2007.
Lucey, D., Hadjiiski, L., Hopke, P. K., Scudlark, J. R., and Church, T.: Identification of sources of pollutants in precipitation measured at the mid-Atlantic US coast using potential source contribution function (PSCF), Atmos. Environ., 35, 3979–3986, 2001.
Jacobson, M. Z.: Strong radiative heating due to the mixing state of black carbon in atmospheric aerosols, Nature, 409, 695–697, 2001.
Lin, W., Xu, X., Ge, B., and Zhang, X.: Characteristics of gaseous pollutants at Gucheng, a rural site southwest of Beijing, J. Geophys. Res., 114, D00G14, doi:10.1029/2008JD010339, 2009.
Liu, P., Zhao, C., Zhang, Q., Deng, Z., Huang, M., Ma, X., and Tie, X.: Aircraft study of aerosol vertical distributions over Beijing and their optical properties, Tellus B, 61, 756–767, 2009.
Ma, J. and van Aardenne, J. A.: Impact of different emission inventories on simulated tropospheric ozone over China: a regional chemical transport model evaluation, Atmos. Chem. Phys., 4, 877–887, doi:10.5194/acp-4-877-2004, 2004.
Ma, N., Zhao, C. S., Nowak, A., Müller, T., Pfeifer, S., Cheng, Y. F., Deng, Z.Z., Liu, P. F., Xu, W. Y., Ran, L., Yan, P., Göbel, T., Hallbauer, E., Mildenberger, K., Henning, S., Yu, J., Chen, L. L., Zhou, X. J., Stratmann, F., and Wiedensohler, A.: Aerosol optical properties in the North China Plain during HaChi campaign: an in-situ optical closure study, Atmos. Chem. Phys., 11, 5959–5973, doi:10.5194/acp-11-5959-2011, 2011.
Miller, J. M.: A five-year climatology of back trajectories from the Mauna Loa observatory, Hawaii, Atmos. Environ., 15, 1553–1558, 1981.
Mlawer, E. J., Taubman, S. J., Brown, P. D., Iacono, M. J., and Clough, S. A.: Radiative transfer for inhomogeneous atmosphere: RRTM, a validated correlated-*k* model for the longwave, J.

ACPD
11, 31137–31158, 2011

Geophys. Res., 102 (D14), 16663–16682, 1997.
Moody, J. L. and Samson, P. J.: The influence of atmospheric transport on precipitation chemistry at two sites in the midwestern United States, Atmos. Environ, 23, 2117–2132, 1989.
Ramanathan, V. and Carmichael, G.: Global and regional climate changes due to black carbon, Nature Geosci., 1(4), 221–227, 2008.
Seibert, P., Kromp-Kolb, H., Baltensperger, U., Jost, D. T., Schwikowski, M., Kasper, A., and Puxbaum H.: Trajectory analyses of aerosol measurements at high alpine sites, in: Transport and Transformation of Pollutants in the Troposphere, edited by: Borrell, P. M., Borrell, P., Cvitas, T., and Seiler, W., Academic Publishing, Den Haag, 689–693, 1994.
Seinfeld, J. H. and Pandis, S. N.: Atmospheric Chemistry and Physics: from Air Pollution to Climate Change, 2nd Edn., Wiley-Interscience Publication, Malden, MA, USA, 2006.
Stohl, A.: Trajectory statistics-a new method to establish source-receptor relationships of air pollutants and its application to the transport of particulate sulfate in Europe, Atmos. Environ., 30(4), 579–587, 1996.
Stohl, A. and Wotaw, G.: A method for computing single trajectories representing boundary layer transport, Atmos. Environ., 29(22), 3235–3238, doi:10.1016/1352-2310(95)00259-2, 1995.
Streets, D. G., Gupta, S., Waldhoff, S. T., Wang, M. Q., Bond, T. C., and Yiyun, B.: Black carbon emissions in China, Atmos. Environ., 35(x), 4281–4296, 2001.
Tang, G., Li, X., Wang, Y., Xin, J., and Ren, X.: Surface ozone trend details and interpretations in Beijing, 2001–2006, Atmos. Chem. Phys., 9, 8813–8823, doi:10.5194/acp-9-8813-2009, 2009.
Xu, W. Y., Zhao, C. S., Ran, L., Deng, Z. Z., Liu, P. F., Ma, N., Lin, W. L., Xu, X. B., Yan, P., He, X., Yu, J., Liang, W. D., and Chen, L. L.: Characteristics of pollutants and their correlation to meteorological conditions at a suburban site in the North China Plain, Atmos. Chem. Phys., 11, 4353–4369, doi:10.5194/acp-11-4353-2011, 2011.
Zhang, Q., Streets, D. G., Carmichael, G. R., He, K. B., Huo, H., Kannari, A., Klimont, Z., Park, I. S., Reddy, S., Fu, J. S., Chen, D., Duan, L., Lei, Y., Wang, L. T., and Yao, Z. L.: Asian emissions in 2006 for the NASA INTEX-B mission, Atmos. Chem. Phys., 9, 5131–5153, doi:10.5194/acp-9-5131-2009, 2009.

ACPD
11, 31137–31158, 2011

Table 1. Mean, minimum and maximum values of the average emissions during 13 July–14 August 2009 from local Wuqing and Beijing, Tianjin Municipality and several sectors of Hebei Province.

Location	CO (ppb h^{-1})			BC (μg m^{-3} h^{-1})		
	Mean	Min.	Max.	Mean	Min.	Max.
Wuqing	193.52	193.52	193.52	0.93	0.93	0.93
Tianjin*	99.75	25.32	249.06	0.45	0.11	1.41
Beijing	120.50	37.79	368.35	0.76	0.20	2.60
Hebei (Langfang)	151.52	99.47	189.29	0.99	0.51	1.62
Hebei (NE)	74.01	13.58	234.52	0.26	0.07	0.72
Hebei (S: $d < 100$ km)	50.42	26.62	77.32	0.35	0.15	0.52
Hebei (S: $d \geq 100$ km)	44.83	5.75	91.28	0.29	0.03	0.58
Hebei (SW: $d < 100$ km)	56.47	38.15	76.80	0.33	0.18	0.44
Hebei (SW: $d \geq 100$ km)	61.53	9.10	109.95	0.31	0.04	0.70

* In the emission assessment of Tianjin, Wuqing was excluded.

ACPD
11, 31137–31158, 2011

Table 2. Mean, minimum and maximum concentration source contributions and according contribution fractions of local emissions and transport from Beijing, Tianjin Municipality and several sectors of Hebei Province.

Location	BC concentration contribution ($\mu g\,m^{-3}\,day^{-1}$) (Fraction (%))						CO concentration contribution ($ppb\,day^{-1}$) (Fraction (%))					
	Mean		Min.		Max.		Mean		Min.		Max.	
Wuqing	5.69	(45.39)	5.69	(86.07)	5.69	(17.05)	1751.69	(58.66)	1751.69	(90.89)	1751.69	(25.83)
Tianjin*	1.97	(15.75)	0.08	(1.23)	12.30	(36.85)	420.73	(14.09)	18.25	(0.95)	2299.20	(33.91)
Beijing	0.41	(3.30)	0.02	(0.29)	3.02	(9.05)	57.26	(1.92)	3.79	(0.20)	292.67	(4.32)
Hebei (Langfang)	1.41	(11.27)	0.41	(6.14)	2.26	(6.78)	214.76	(7.19)	80.52	(4.18)	321.71	(4.74)
Hebei (NE)	0.11	(0.90)	0.00	(0.05)	0.57	(1.71)	34.68	(1.16)	0.55	(0.03)	266.09	(3.92)
Hebei (S: $d < 100$ km)	1.29	(10.27)	0.24	(3.56)	4.51	(13.52)	186.13	(6.23)	40.45	(2.10)	690.96	(10.19)
Hebei (S: $d \geq 100$ km)	0.19	(1.51)	0.01	(0.19)	0.85	(2.55)	27.99	(0.94)	2.42	(0.13)	100.80	(1.49)
Hebei (SW: $d < 100$ km)	1.23	(9.81)	0.16	(2.38)	3.16	(9.47)	252.10	(8.44)	27.44	(1.42)	905.90	(13.36)
Hebei (SW: $d \geq 100$ km)	0.23	(1.80)	0.01	(0.09)	1.01	(3.02)	40.88	(1.37)	2.11	(0.11)	151.84	(2.24)

* In the contribution assessment of Tianjin, Wuqing was excluded.

ACPD
11, 31137–31158, 2011

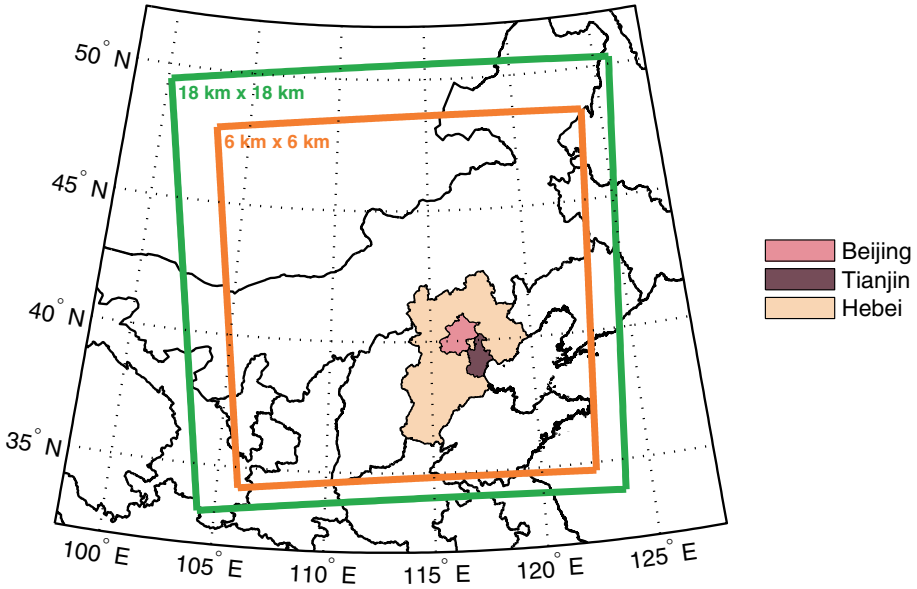

Fig. 1. Model domains for the ARW meteorology simulations and the locations of Beijing and Tianjin Municipality and Hebei Province. The green box shows the coarse domain at 18 km spatial resolution and the orange box shows the finer domain at 6 km spatial resolution.

ACPD
11, 31137–31158, 2011

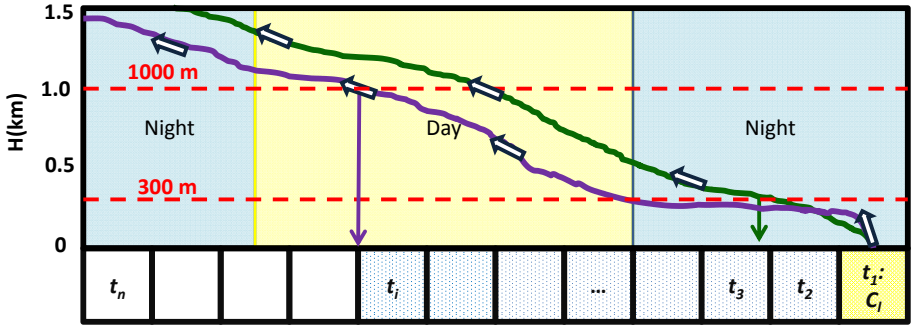

Fig. 2. Schematic showing the determination of the PBL residence time of trajectories, where $t_1 - t_n$ stand for the time points associated with the n endpoints of trajectory l, C_l is the concentration observed at t_1 (upon arrival of l). The green and purple line show example trajectories, that exceed the boundary layer height during night time and daytime, respectively.

ACPD
11, 31137–31158, 2011

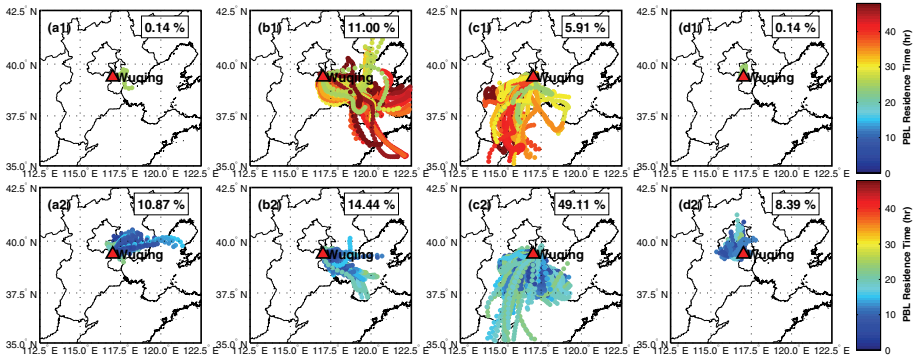

Fig. 3. Cluster frequency analyses of trajectories during 13 July–14 August 2009 in the North China Plain, **(a–d)** stand for the average directions N–E, S–E, S–W and N–W, respectively, the upper 4 panels display trajectories with PBL residence time longer than 24 h, while the lower panels show those with PBL residence time below 24 h.

ACPD
11, 31137–31158, 2011

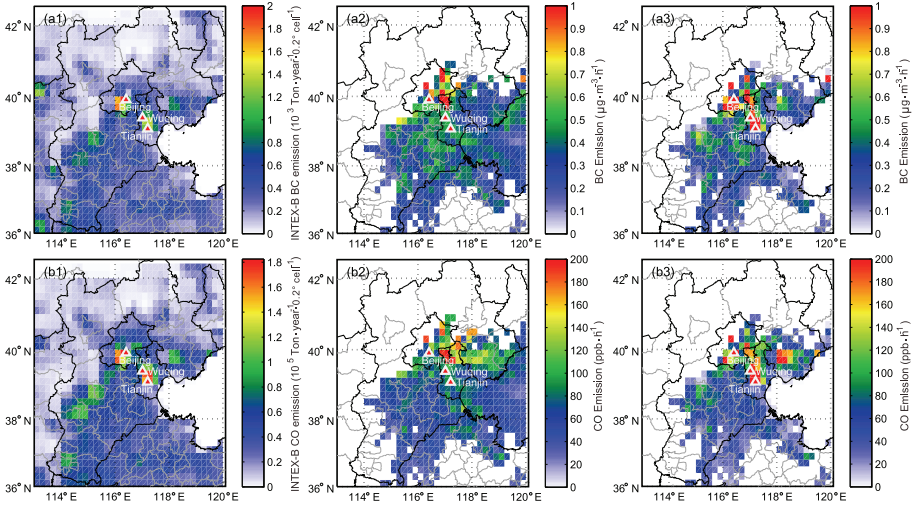

Fig. 4. 2006 INTEX-B total emission inventory of BC **(a1)** and CO **(b1)** and estimated mean emission field of BC **(a2, a3)** and CO **(b2, b3)** during 13 July–14 August 2009 in the North China Plain. The second column represents the derived emission fields without the INTEX-B inventory as weighting factor, while the third column represents the results after using the weighting factor.

ACPD
11, 31137–31158, 2011